Biochemistry

 Volume 42, Number 38 September 30, 2003

Accelerated Publications

Crystal Structure of Fucose-Specific Lectin from *Aleuria aurantia* Binding Ligands at Three of Its Five Sugar Recognition Sites[†,‡]

Masahiro Fujihashi,[§,||] Diane Hope Peapus,[§,⊥] Nobuo Kamiya,[@] Yoshiho Nagata,[#] and Kunio Miki*[,§,@]

Department of Chemistry, Graduate School of Science, Kyoto University, Sakyo-ku, Kyoto 606-8502, Japan, RIKEN Harima Institute/SPring-8, Koto 1-1-1, Mikazukicho, Sayo-gun, Hyogo 679-5148, Japan, and Department of Bioresources Chemistry, Faculty of Horticulture, Chiba University, Matsudo 271-8510, Japan

Received June 9, 2003; Revised Manuscript Received August 10, 2003

ABSTRACT: *Aleuria aurantia* possesses a fucose-specific lectin (AAL) that is widely used as a specific probe for fucose. Fucosylated sugars often play pivotal roles in many cellular processes. We have determined the crystal structure of AAL at 2.24 Å resolution in complex with only three fucose molecules in its five sugar binding sites of a six-fold β-propeller structure. Very recently, the structure of AAL has been independently determined, showing that all the five binding sites were occupied by fucose molecules [Wimmerova, M., *et al*. (2003) *J. Biol. Chem. 278*, 27059−27067]. Stabilization of the arginine conformation bound to fucose molecules plays an essential role in generating the difference in the affinity in the five binding sites. Binding models with a couple of saccharides based on biochemical assays suggest that hydrophobic contacts also play important roles in AAL recognizing its ligand.

Lectins are sugar-binding proteins, some of which have great value as specific probes for investigating the structure and function of carbohydrate chains on glycoproteins and glycolipids. Many kinds of lectins are found in plants, animals, and fungi; more than 200 crystal structures have been determined. These structures are classified into various folding families, such as legume lectin folding, C-type lectin, I-type lectin, P-type lectin, β-prism I and II, β-trefoil, five-β-propeller folding, etc. (*1*). Most of these families contain several β-strands in the core structure. The most widely observed folding is the legume lectin folding which consists of a two-layered β-sheet structure termed the jellyroll motif (*1*).

The carbohydrate moieties of glycoproteins and glycolipids on cell surfaces have been shown to be involved in a variety of biological recognition processes, including cell−cell interactions, cell−substratum interactions, metastasis of tumor cells, etc. (*2*). α-L-Fucopyranosyl residues are widely distributed in cell-surface sugar chains, and in many cases, the residues constitute parts of important antigens such as the blood group antigen H (*3*) and the stage-specific embryonic antigens (*4*). Among various lectins, crystal structures of three kinds of fucose-specific lectins have been

[†] This work was supported in part by the "Research for the Future" Program from the Japan Society for the Promotion of Science (JSPS-RFTF 97L00501 to K.M.) and Grant-in-Aid for Scientific Research 02660080 from the Ministry of Education, Science, Sports and Culture, Japan (to Y.N.). D.H.P. was supported by Postdoctoral Fellowships for Foreign Researchers P95213 and P97006 and STA Short Term Fellowship 398057 from the Japan Society for the Promotion of Science (JSPS), and by National Science Foundation Grant-in-Aid of JSPS Fellows INT-9512766.

[‡] The atomic coordinates of AAL have been deposited in the Protein Data Bank as entries 1IUC and 1IUB for the native and the Hg derivative crystals, respectively.

* To whom correspondence should be addressed. Telephone: +81-75-753-4029. Fax: +81-75-753-4032. E-mail: miki@kuchem.kyoto-u.ac.jp.

[§] Kyoto University.

[||] Present address: Division of Molecular and Structural Biology, Ontario Cancer Institute, University Health Network, 610 University Ave., Toronto, Ontario M5G 2M9, Canada.

[⊥] Present address: Paleontological Research Institution, 1259 Trumansburg Rd., Ithaca, NY 14850.

[@] RIKEN Harima Institure/SPring-8.

[#] Chiba University.

10.1021/bi034983z CCC: $25.00
Published on Web 09/05/2003

Table 1: Data Collection and Phasing Statistics

	native	edge	peak	remote
wavelength (Å)	1.000	1.0090	1.0039	0.9183
resolution (Å)[a]	100−2.24 (2.29−2.24)	200−2.49 (2.55−2.49)	200−2.48 (2.54−2.48)	200−2.31 (2.36−2.31)
R_{merge} (%)[a]	6.1 (30.1)	5.4 (19.6)	6.4 (16.9)	6.7 (29.0)
completeness (%)[a]	91.2 (81.2)	95.5 (79.2)	96.2 (95.0)	95.4 (93.0)
phasing power (acentric/centric)		−	1.31/0.86	1.51/1.05
mean figure of merit		0.696		

[a] Values in parentheses are for the outermost resolution shell.

determined. A legume lectin from *Ulex europeus* (UEA-I) exhibited a first crystal structure in these lectins (*5*). The structure has a common legume lectin folding which is similar to those of other legume lectins, including those with no fucose binding activity. The second and third structures were determined in 2002 with their ligand fucose molecules. The structure of *Anguilla anguilla* agulutinin (AAA), which was isolated from the serum of eel, indicates AAA folds as a β-barrel with a jellyroll topology (*6*). The structure of a bacterial lectin from *Pseudomonas aeruginosa* (PA-IIL) has nine β-strands containing a Greek-key motif (*7*). A fucose molecule is bound to a loop region with two calcium ions. The binding modes in these three lectins are different from each other. Very recently, the fourth crystal structure of fucose-specific lectin from *Aleuria aurantia* (AAL)[1] has been determined by Wimmerova *et al.* (*8*). It was shown that AAL has a six-fold β-propeller structure and forms six clefts between each blade. The ligand fucose molecules are found in five of six clefts in a monomer, whereas only one fucose binding site in a monomer has been found in three other fucose-specific lectins.

We have independently determined the structure of AAL using the crystal with a different space group (*9*). The overall protein structure looks identical to that determined by Wimmerova *et al.* (*8*). However, only three fucose molecules are found in the AAL monomer of our structure, suggesting differences in the binding affinity in five sugar binding sites. Here we report the independently determined crystal structure of AAL at 2.24 Å resolution and discuss the difference in the recognition modes at each binding site.

MATERIALS AND METHODS

Purification, Crystallization, and Data Collection. Recombinant AAL was purchased from Nichirei Co. Ltd. (Tokyo, Japan), which was overexpressed in *Escherichia coli* and purified using a fucose-starch column (*10*, *11*). Elution from the column was performed with phosphate-buffered saline (PBS) containing 50 mM L-fucose. Afterward, the 25 mL AAL fraction was dialyzed twice against 2 L of PBS. Crystallization of native AAL and cocrystallization with mercury chloride were carried out as described previously (*9*). X-ray diffraction data from the native crystals and Hg cocrystals were collected at room temperature at the Photon Factory (BL18B) and ESRF (BM14), respectively. The diffraction data were reduced using DENZO, SCALEPACK (*12*), and TRUNCATE (Table 1) (*13*). Both crystals belong to space group $P6_522$. The cell parameters of the native crystals are as follows: $a = 84.0$ Å and $c = 250.1$ Å (*9*). Those of the Hg cocrystals are as follows: $a = 83.9$ Å and $c = 254.3$ Å (*9*). On the other hand, the crystals of AAL used by Wimmerova *et al.* belong to space group $P2_1$ with the following unit cell parameters: $a = 46.0$ Å, $b = 86.4$ Å, $c = 77.9$ Å, and $\beta = 90.6°$ (*8*).

[1] Abbreviation: AAL, *A. aurantia* lectin.

Table 2: Refinement and Model Statistics

	native	Hg cocrystal (remote data)
resolution (Å)[a]	40−2.24 (2.38−2.24)	40−2.31 (2.45−2.31)
R (%)[a]	16.5 (20.7)	16.1 (21.2)
R_{free} (%)[a]	19.6 (23.0)	18.3 (24.1)
no. of reflections[b]	46425	43442
no. of atoms	2577	2515
AAL	2369	2372 (AAL + 2Hg + 1Cl)
fucose	33 (three molecules)	22 (two molecules)
sulfate	5 (one molecule)	5 (one molecule)
water	170	116

[a] Values in parentheses are for the outermost resolution shell. [b] Bijvoet pairs are counted as two reflections.

Phasing and Model Building. Because the length of the *c*-axis of the native crystals is much different from that of the Hg cocrystals, the structure was determined using the multiwavelength anomalous diffraction method with MLPHARE (*13*) using three wavelength data sets from a single Hg cocrystal (Table 1). The edge data with the lowest f' were used as a reference data set. Experimental phases were improved by solvent flattening, histogram matching, and multiresolution modification using the program DM (*13*). The electron density maps of the Hg cocrystals with improved phases were good enough that all residues could be traced. The structural model in the Hg cocrystal was constructed using the program O (*14*), and refined using the program CNS (*15*) against the remote data set that had the highest resolution among the three MAD data sets (Table 2). Two mercury atoms were bound to two cysteine residues in an AAL subunit. No restraints were applied for these mercury atoms during the CNS refinement step. After the model building of an Hg-bound AAL structure was completed, an Hg-free AAL model was constructed and refined using the native (Hg-free) data set using the same refinement strategy that was used for the Hg cocrystal. At the final stage of the refinement, the occupancy values of fucose molecules and *B*-factors of the entire molecule were alternately refined until both values become stable at 2.24 and 2.31 Å resolutions for the native and Hg cocrystal structures, respectively (Table 2). Secondary structures were determined using the program PROCHECK based on the main chain conformation. The three-dimensional superimpositions were performed using the program LSQMAN (*16*).

RESULTS AND DISCUSSION

Overall Structure. The overall structure of AAL is shown in Figure 1. All 312 amino acid residues are well-refined.

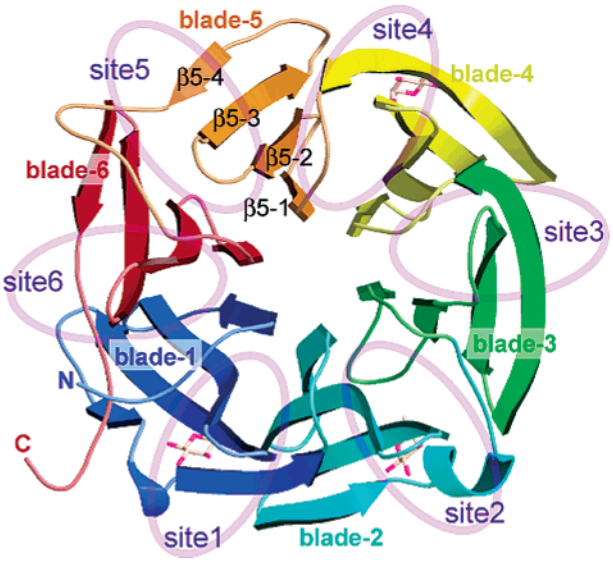

FIGURE 1: Overall structure of the AAL monomer. Blue, cyan, green, yellow, orange, and red ribbons show blades 1−6, respectively. Purple ellipsoids indicate fucose binding sites 1−5 and the corresponding site 6. Three stick models at sites 1, 2, and 4 show fucose molecules. This figure was prepared using Molscript (*26*) and Raster3D (*27*).

Our structure looks identical to the structure determined by Wimmerova *et al.* (*8*). The folding is classified as a six-fold β-propeller protein, and almost all secondary structures are β-strands and loops. Two 3_{10}-helices are found; one is inserted in the outmost strand in blade 1, and the other is located in the loop between blades 2 and 3.

No lectins have been found in known six-fold β-propeller proteins, although a couple of structures are available in this family, including phytase, glucose dehydrogenase, *E. coli* TolB protein, and low-density lipoprotein (LDL) receptor (*17*−*20*). Apparently, AAL is the first example of a lectin composed of a six-fold β-propeller. Almost all residues of AAL are used to form the propeller structure, whereas all other known six-blade proteins possess an other domain(s) or large loop region(s) (*21*). AAL forms the most compact structure among all known six-blade proteins.

AAL forms a dimeric form in the crystal presented here as observed in the crystal by Wimmerova *et al.* (*8*), which coincides the observations from sedimentation equilibrium and gel filtration under a physiological condition (*22*). The asymmetric unit in the crystal presented here contains only a monomer molecule of AAL, and the dimer is located on a crystallographic two-fold axis, which relates two monomers in different crystallographic asymmetric units. 7.7% of the monomer surface contacts the other monomer to form the physiological dimer in this crystal. This rate is relatively low, but still 1.6 times higher than that of the second largest contact. The small interface in the physiological dimer may cause the high solvent content (68%) of this crystal (*9*).

Fucose Molecules Are Found in Only Three of Five Sites. Surprisingly, only three firmly bound fucose molecules were found in our crystal structure (Figure 2A), whereas five molecules are found in the structure of a different crystal (*8*). These fucose molecules are located at site 1 (between blades 1 and 2), site 2 (blades 2 and 3), and site 4 (blades 4 and 5) (Figure 1). The fucose molecules in sites 1 and 2 are β-anomers (equatorial O1), and that in site 4 is an α-anomer (axial O1). As discussed later, site 6 is not a binding site, which is consistent with the fact that no ligands are found at site 6 in the other crystal structure (*8*). No electron

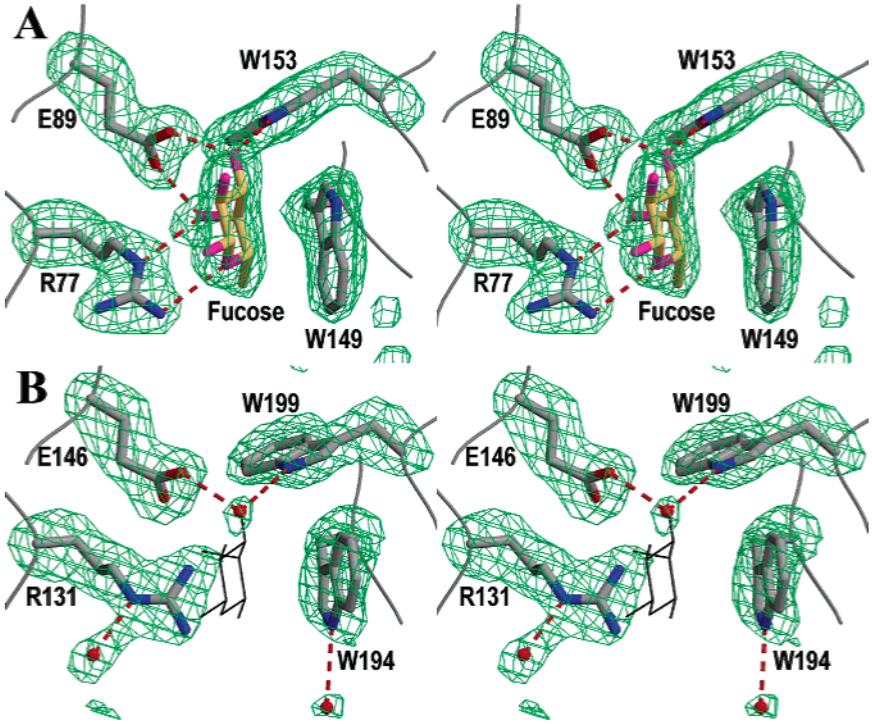

FIGURE 2: Stereoviews of sites 2 and 3 with an $F_o - F_c$ omit electron density map. Red dashed lines represent hydrogen bonds. This figure was prepared using Molscript (*26*), Conscript (*28*), and Raster3D (*27*). (A) Site 2. The side chains of R77, E89, W149, and W153 as well as the fucose molecule have been omitted in the phase calculation. (B) Site 3. Black bonds represent a corresponding fucose binding position estimated from sites 1, 2, and 4. There is no electron density for fucose. Red spheres represent water molecules. The side chains of R131, E146, W194, and W199 as well as the water molecules have been omitted in the phase calculation.

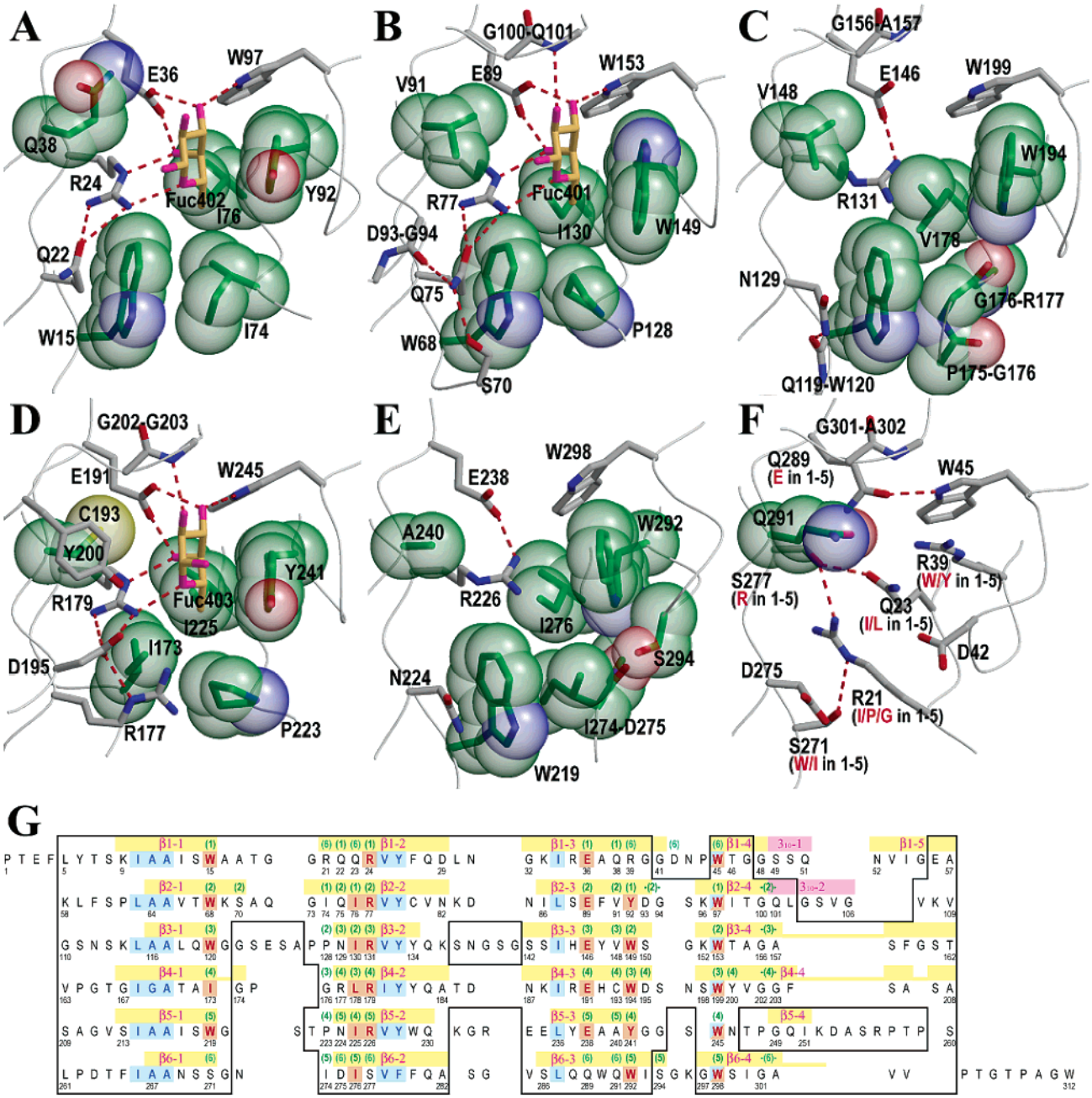

FIGURE 3: (A−F) Close-up view of each fucose binding site: (A) site 1, (B) site 2, (C) site 3, (D) site 4, (E) site 5, and (F) site 6. Gray wires trace the peptide backbones. Green atoms show carbons bound to the fucose molecule with hydrophobic interactions. Yellow, red, and blue atoms represent sulfur, oxygen, and nitrogen, respectively. Red dashed lines represent hydrogen or ionic bonds. Panels A−F were prepared using Molscript (*26*) and Raster3D (*27*). (G) Sequence alignments of six tandem repeats of AAL. Black line boxes denote well-superimposed residues on the basis of the crystal structure. Residues colored blue are conserved in all six repeats and form a hydrophobic core structure of six β-propellers. Residues colored red form the fucose binding sites and are conserved in at least five repeats. Numbers in parentheses and colored green indexed at the upper side of sequences show the site numbers. Secondary structures are shown with yellow (β-strands) and light magenta (3_{10}-helices) bold bars with dark magenta labels.

densities except for those corresponding to waters are found at sites 3 and 5 (Figure 2B). Fucose molecules are found at both sites in the other crystal structure (*8*).

We had never employed any saccharide reagents during the crystallization steps of AAL. The fucose molecules found in the crystal structure must come from the 50 mM fucose solution used as an elution buffer of the affinity column in the purification step (*10*). Despite two subsequent steps of dialysis against a fucose-free buffer to the affinity column, these fucose molecules were not dissociated from AAL. This indicates that sites 1, 2, and 4 can recognize fucose molecules in an ~0.05 mM solution (*10*).

Sequence Alignment Based on the Three-Dimensional Structure. The superimposition of the six sites of the β-propeller motif shows that the characteristic residues at sites 1−5 superimpose well, including arginine, glutamic acid, and tryptophan which form hydrogen bonds with fucose, in addition to aromatic residues, tryptophan and tyrosine (Figure 3A−E), except for site 6 (Figure 3F). The six tandem repeats in the primary structure of AAL (*23*) were

realigned on the basis of the three-dimensional structure (Figure 3G).

Some residues are conserved in five of six tandem repeats except for the residues forming site 6, whereas some are conserved in all six repeats. Amino acids conserved at five of the six sites, which are highlighted with red in Figure 3G, are located on the surface of the AAL and directly contribute to fucose recognition. Because the corresponding residues forming site 6 are not conserved, this site cannot be considered to accommodate fucose molecules. On the other hand, residues conserved in all six blades (highlighted with blue in Figure 3G) form a hydrophobic core of the AAL structure. These residues are indispensable in maintaining the six-fold β-propeller structure as seen in the other β-propeller proteins (*21*). Conserved tryptophans on the outermost strand (W97, W153, W199, W245, W298, and W45) contribute both to form the hydrophobic core and to recognize fucose molecules.

Differences of Each Site. The five fucose binding sites are structurally very similar to each other. However, fucose molecules are found only at sites 1, 2, and 4 in the crystal structure. No monosaccharides are found at sites 3 and 5.

The guanidinium groups of R131 and R226 in sites 3 and 5 are pointing toward the right side in the orientation shown in panels C and E of Figure 3, respectively. These guanidinium groups occupy binding sites 3 and 5. On the other hand, the guanidinium groups of R24 and R77 at sites 1 and 2 form hydrogen bonds with Oϵ1 of Q22 and Q75, respectively (panels A and B of Figure 3, respectively). These hydrogen bonds turn the guanidinium groups toward the left side and keep the fucose binding sites open. The side chains of glutamines Q22 and Q75 take staggered conformations, which are energetically stable. The corresponding residues to these glutamines are N129 and N224 at sites 3 and 5, respectively. Because the number of carbons in the side chain in asparagine is just one less than that of glutamine, R131 and R226 cannot form hydrogen bonds with these asparagines (N129 and N224) without energetically unstable eclipsed conformations. Instead of forming the bonds with these asparagines, R131 and R226 form ionic bonds with E146 and E238, respectively. These ionic bonds make the guanidinium groups of these arginines occupy the fucose binding sites.

At fucose binding site 4, R177 corresponds to Q22 in site 1 (panels A and D of Figure 3, respectively). A neighbor residue D195 forms ionic bonds with both R177 and R179. The ionic bond between D195 and R179 also keeps site 4 open. These two ionic bonds are also found in the mercury derivative structure of AAL. In the derivative structure, a mercury atom, which binds to C193 at site 4, prevents the fucose molecule from binding at this site because of steric hindrance. The mercury atom does not so much affect the conformation of the guanidinium group of R179, because the distances between the mercury and the guanidinium groups in the left (open fucose binding site) and right (occupied fucose binding site) conformers are almost the same. This suggests the ionic bond between D195 and R177 is strong enough to keep fucose binding site 4 open without any fucose molecules.

The occupancy values of the fucose molecules are 81, 100, and 93% at sites 1, 2, and 4, respectively. Six hydrogen bonds are found between fucose and AAL at sites 2 and 4, whereas five are found at site 1. The hydrogen bonds with the main chain N atoms of Q101 (site 2) and G203 (site 4) may contribute to strengthening of fucose binding.

In some case, crystallographic contacts may affect binding geometries between a protein molecule and its ligand(s). Site 3 is far away from such contacts in our crystal structure. This indicates the affinity of site 3 is weaker than those of sites 1, 2, and 4. A couple of residues at site 5 are related to the crystallographic contact. However, as mentioned above and shown in Figure 3A−F, the structural features of site 5 are very similar to those of site 3. Sites 3 and 5 are considered not to have accommodated fucose molecules even at the beginning of the crystallization, because we have never used any fucose-containing solutions to handle the crystals. These suggest the binding affinity of site 5 is close to that of site 3. Consequently, it could be concluded that sites 2 and 4 are strong binding sites, site 1 may be medium in strength, sites 3 and 5 are relatively weak, and site 6 is not a fucose binding site.

Site 6 might have lost its ability to accommodate the ligand during the evolutional process, probably because of a requirement for protein folding. Four hydrogen bonds shown in Figure 3F connect two blades around site 6, whereas no corresponding bonds are found in sites 1−5 (Figure 3A−E). Site 6 is located between blades 1 and 6, implying a role in connecting the first and last blades to stabilize the six-fold β-propeller structure.

Specificity for Several Sugars. AAL recognizes D-arabinose that lacks the C6 methyl group of L-fucose (*10*, *24*). The affinity of binding to arabinose is 30 times weaker than the affinity of binding to L-fucose. Figure 4A shows a binding model of AAL with D-arabinose. The hydrophobic pocket located on the lower side in the figure is vacant when D-arabinose binds AAL. This shows the methyl group recognition pocket strongly contributes to fucose recognition. AAL also binds methyl α-L-fucoside 8 times stronger, and methyl α-L-fucoside has an additional methyl group on O1 of α-L-fucose, compared to L-fucose (*22*). The additional methyl group can form a hydrophobic contact with the aromatic ring located on the right side as shown in a binding model in Figure 4B. These facts indicate that not only the hydrogen bonds but also the hydrophobic contacts play essential roles in recognition of fucose molecules.

The α-(1−6)-linked L-fucopyranosyl group is the best ligand for AAL among α-(1−2)-, α-(1−3)-, α-(1−4)-, and (1−6)-linked L-fucopyranosyl groups (*23*, *25*). These oligosaccharides have a covalent bond between the O1 atom of fucose and an atom of the other sugar. Because α-(1−6)-fucopyranose has two atoms between the ring of fucose and the next sugar whereas other fucopyranoses have only one atom between the two rings, the conformational flexibility of α-(1−6)-fucopyranose is thought to be higher than those of other fucopyranoses. Thus, α-(1−6)-fucopyranose can easily take an appropriate conformation to avoid steric hindrance with AAL. The importance of the conformational flexibility is also found in the analysis with oligosaccharides having two fucose residues (*23*, *25*). Such oligosaccharides bind AAL stronger than that with only one fucose residue. It is too far for such oligosaccharides to bind at two neighbor binding sites on AAL. This can be explained if either of two fucose residues may have an appropriate conformation for binding AAL. In addition, monosaccharide L-fucose can

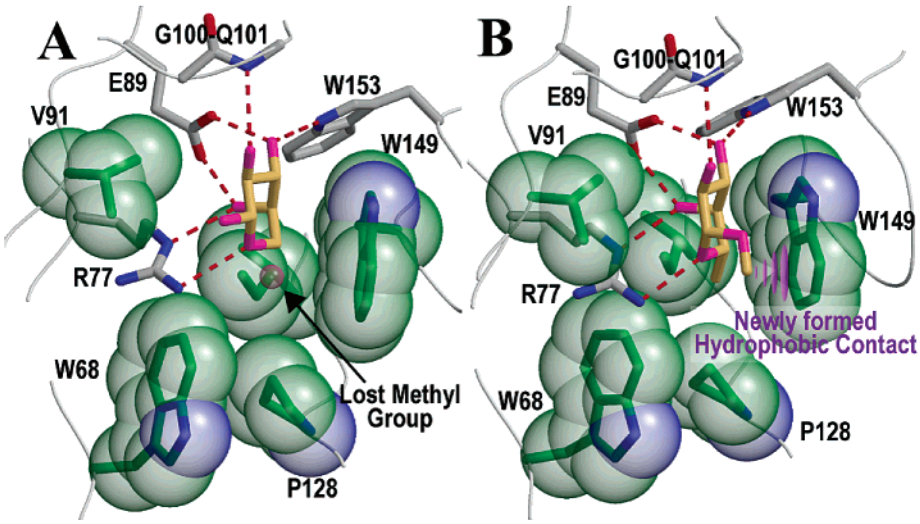

FIGURE 4: Hypothetical binding models with various ligand molecules. The color scheme is the same as that in panels A−F of Figure 3. (A) D-Arabinose at site 2. (B) Methyl α-L-fucoside at site 2. This figure was prepared using Molscript (*26*) and Raster3D (*27*).

bind AAL stronger than large oligosaccharides (more than three residues) with fucose residues (*23*, *25*). These facts suggest that AAL recognizes only one fucose residue in an oligosaccharide.

We have determined the crystal structure of the commercially available AAL without addition of any saccharide reagents. All commercial AALs are produced by the same protocol that we employed in this study, in which the most essential step is fucose−starch column chromatography. Therefore, such commercial AALs may also contain fucose molecules at the binding sites. However, many biochemical experiments show that such AALs can maintain their lectin activities (*10*, *11*). Three reasons for this can be proposed. First, the four unoccupied binding sites in dimeric AAL recognize their ligand molecules. Second, the concentration of ligands used in such biochemical experiments is high enough to replace the originally bound fucose molecules. Third, the affinity of binding of some oligosaccharides to AAL, such as an α-(1−6)-linked L-fucopyranosyl group, is stronger than that of a monosaccharide fucose. If the fucose molecules could be removed from the binding sites of AAL, the lectin might recognize the ligands with higher sensitivity.

The multiplicity of the fucose binding sites may allow AAL to bind various kinds of oligosaccharides. The slight structural difference at the five binding sites may enable the AAL molecule to avoid steric hindrance with various ligands. In addition, though only one site can recognize an oligosaccharide, the dimeric AAL can provide two binding sites for the ligand and hemagglutinin activity. The wide specificity may contribute to the defense for the host organism from the various kinds of mold and bacteria. More detailed experiments are necessary to clarify the significance of differences in recognition affinity among five sites and to understand how the multiplicity and the variety of recognition sites control the binding activity in living cells.

ACKNOWLEDGMENT

We thank Drs. N. Sakabe, N. Watanabe, M. Suzuki, N. Igarashi, and A. Thompson for their help in diffraction studies at the Photon Factory (Proposals 90-184, 92G218, and 94G254) and at ESRF (Proposal LS-804). K.M. is a member of the Structural Biology Sakabe Project of the Photon Factory. We are also indebted to Drs. A. Ando, Y. Sugawara, Y. Higuchi, A. Kita, J. Saito, T. Fukami, and T. Nogi for their contributions in sample preparation, crystallization, and data collection.

REFERENCES

1. Vijayan, M., and Chandra, N. (1999) *Curr. Opin. Struct. Biol. 9*, 707−714.
2. Drickamer, K., and Taylor, M. E. (1993) *Annu. Rev. Cell Biol. 9*, 237−264.
3. Hakomori, S., and Kobata, A. (1974) in *The Antigens* (Sela, M., Ed.) Vol. 2, pp 79−140, Academic Press, New York.
4. Stelck, S., Robitzki, A., Willbold, E., and Layer, P. G. (1999) *Glycobiology 9*, 1171−1179.
5. Audette, G. F., Vandonselaar, M., and Delbaere, L. T. (2000) *J. Mol. Biol. 304*, 423−433.
6. Bianchet, M. A., Odom, E. W., Vasta, G. R., and Amzel, L. M. (2002) *Nat. Struct. Biol. 9*, 628−634.
7. Mitchell, E., Houles, C., Sudakevitz, D., Wimmerova, M., Gautier, C., Perez, S., Wu, A. M., Gilboa-Garber, N., and Imberty, A. (2002) *Nat. Struct. Biol. 9*, 918−921.
8. Wimmerova, M., Mitchell, E., Sanchez, J. F., Gautier, C., and Imberty, A. (2003) *J. Biol. Chem. 278*, 27059−27067.
9. Fujihashi, M., Peapus, D. H., Nakajima, E., Yamada, T., Saito, J. I., Kita, A., Higuchi, Y., Sugawara, Y., Ando, A., Kamiya, N., Nagata, Y., and Miki, K. (2003) *Acta Crystallogr. D59*, 378−380.
10. Fukumori, F., Takeuchi, N., Hagiwara, T., Ohbayashi, H., Endo, T., Kochibe, N., Nagata, Y., and Kobata, A. (1990) *J. Biochem. 107*, 190−196.
11. Nagata, Y., Fukumori, F., Sakai, H., Hagiwara, T., Hiratsuka, Y., Kochibe, N., and Kobata, A. (1991) *Biochim. Biophys. Acta 1076*, 187−190.
12. Otwinowski, Z., and Minor, W. (1997) *Methods Enzymol. 276*, 307−326.
13. Collaborative Computional Project, Number 4 (1994) *Acta Crystallogr. D50*, 760−763.
14. Jones, T. A., Zou, J.-Y., and Cowan, S. W. (1991) *Acta Crystallogr. A47*, 110−119.
15. Brünger, A. T., Adams, P. D., Clore, G. M., DeLano, W. L., Gros, P., Grosse-Kunstleve, R. W., Jiang, J. S., Kuszewski, J., Nilges, M., Pannu, N. S., Read, R. J., Rice, L. M., Simonson, T., and Warren, G. L. (1998) *Acta Crystallogr. D54*, 905−921.
16. Kleywegt, G. J. (1996) *Acta Crystallogr. D52*, 842−857.
17. Kostrewa, D., Gruninger-Leitch, F., D'Arcy, A., Broger, C., Mitchell, D., and van Loon, A. P. (1997) *Nat. Struct. Biol. 4*, 185−190.

18. Oubrie, A., Rozeboom, H. J., Kalk, K. H., Olsthoorn, A. J., Duine, J. A., and Dijkstra, B. W. (1999) *EMBO J. 18*, 5187−5194.
19. Abergel, C., Bouveret, E., Claverie, J. M., Brown, K., Rigal, A., Lazdunski, C., and Benedetti, H. (1999) *Struct. Folding Des. 7*, 1291−1300.
20. Jeon, H., Meng, W., Takagi, J., Eck, M. J., Springer, T. A., and Blacklow, S. C. (2001) *Nat. Struct. Biol. 8*, 499−504.
21. Paoli, M. (2001) *Prog. Biophys. Mol. Biol. 76*, 103−130.
22. Kochibe, N., and Furukawa, K. (1980) *Biochemistry 19*, 2841−2846.
23. Yamashita, K., Kochibe, N., Ohkura, T., Ueda, I., and Kobata, A. (1985) *J. Biol. Chem. 260*, 4688−4893.
24. Ogawa, S., Otta, Y., Ando, A., and Nagata, Y. (2001) *Biosci., Biotechnol., Biochem. 65*, 686−689.
25. Debray, H., and Montreuil, J. (1989) *Carbohydr. Res. 185*, 15−26.
26. Kraulis, P. J. (1991) *J. Appl. Crystallogr. 24*, 946−950.
27. Merritt, E. A., and Bacon, D. J. (1997) *Methods Enzymol. 277*, 505−524.
28. Lawrence, M. C., and Bourke, P. (2000) *J. Appl. Crystallogr. 33*, 990−991.

BI034983Z